

# Residual stress in thin films PECVD depositions: a review

C. ILIESCU, M. AVRAM<sup>a</sup>, B. CHEN, A. POPESCU<sup>a</sup>, V. DUMITRESCU<sup>a</sup>, D. P. POENAR<sup>c</sup>, A. STERIAN<sup>b</sup>, D. VRTACNIK<sup>d</sup>, S. AMON<sup>d\*</sup>, P. STERIAN<sup>b</sup>

*Institute of Bioengineering and Nanotechnology, Singapore,*

<sup>a</sup>*National Institute for Research and Development in Microtechnologies, Romania*

<sup>b</sup>*Nanyang Technological University, Singapore, School of Electrical Engineering*

<sup>c</sup>*University "Politehnica" of Bucharest, Dept. of Physics, Romania*

<sup>d</sup>*University of Ljubljana, Faculty of Electrical Engineering, Laboratory of Microsensor Structures and Electronics, Slovenia*

The paper presents solutions for residual stress control in thin films deposition on plasma enhanced chemical vapor depositions (PECVD) reactors and some MEMS applications. The residual stress induced in the thin films is an important factor in the fabrication of thin and free standing MEMS structure such as membranes or cantilevers fabricated using surface or bulk micromachining. The main layers analyzed are: amorphous silicon, amorphous silicon carbide and amorphous silicon nitride. The main parameters analyzed are the temperature of the deposition process, pressure, gas composition, as well as the value of the power and the power mode (high frequency - 13.56 MHz or low frequency - 400 KHz). Due to annealing effect, the temperature can decrease the compressive value of the stress. The RF frequency mode presents a major influence of residual stress: in low frequency mode a relatively high compressive stress is achieved due to ion bombardment and, as a result, densification of the layer is achieved.

(Received March 9, 2011; accepted April 15, 2011)

**Keywords:** PECVD, Low stress, Silicon nitride,  $\alpha$ -Si:H,  $\alpha$ -SiC

## 1. Introduction

The paper reports new fabrication methods for low stress silicon nitride ( $\text{SiN}_x$ ), amorphous silicon ( $\alpha$ -Si:H) and amorphous silicon carbide ( $\alpha$ -SiC) layers at high deposition rates in a PECVD reactor. Silicon nitride ( $\text{SiN}_x$ ) is one of the widely used materials in semiconductor technology, miniature devices and biomedical applications. It can be used for passivation, insulation, mechanical protection, as well as masking layer for anisotropic etching of silicon in alkaline solutions and capping layer during implantation [1]. Moreover, due to its fracture toughness, high wear resistance and biocompatibility [2, 3], silicon nitride is considered as a biomaterial for orthopedic and dental implants. Low stress  $\text{SiN}_x$  layer has wide applications such as diaphragm in single-wafer fabricated silicon condenser microphone [4], 3-D passivation layer for planar sensors [5], hardmasks on SRAM X-ray masks [6], optical MEMS - Fabry-Pérot filter and vertical cavity surface emitting laser - [7,8] and suspensions in micromachined silicon accelerometers [9]. In order to achieve stress reduction of  $\text{SiN}_x$  layer, many processes have been developed. Tarraf et al [10] and van de Ven et al [11] used low and high RF frequency mix, which applications,  $\alpha$ -Si alternatively applied low and high frequency, consequently compensating the tensile stress from high frequency (HF) by compressive stress from low frequency (LF) to produce low stress silicon nitride. Mackenzie et al [12] adjusted the stress of  $\text{SiN}_x$  through the addition of He to the standard gas

mixture of  $\text{SiH}_4$ ,  $\text{NH}_3$  and  $\text{N}_2$ . By changing the ratio of  $\text{N}_2$  and He, they achieved the stress from 300 MPa tensile through zero to about - 300 MPa, compressive. Loboda and Seifferly [13] introduced Ar into the process as a diluting gas. They found that when Ar was added, Si-H<sub>x</sub> plasma chemistry and film hydrogen bond density changed, producing a reduction in the amount of tensile stress. Previous reports regarding the impact of high RF power on  $\text{SiN}_x$  layer are reported by Wu et al [14] and Sleenckx et al [15]. Amorphous silicon ( $\alpha$ -Si:H) thin films are often used in diverse sensing and MEMS applications. It can be a structural layer of thin film devices, such as photodiodes [16] or thin film transistors for color [17] or infrared sensing [18], piezoresistors for pressure sensor fabricated on a flexible membrane [19] or can be used to form micromechanical beams [20]. Due to its good resistance in highly concentrated HF solutions [21], the  $\alpha$ -Si:H films are often used as masking layers for glass etching in microfluidic applications [22, 23], or even as thin electrodes in a dielectrophoretic chip [24]. In other: H serves as sacrificial layer in the microfabrication of capacitive ultrasonic transducers [25] due to its easy removal by wet etching in an alkaline solution (TMAH or KOH). Alternatively, a dry-release process in  $\text{XeF}_2$  of  $\alpha$ -Si:H nano-films was used to define a nano-gap in piezoelectric resonators for mechanical RF magnetic field modulation [26].  $\alpha$ -Si:H can also be used as interlayer for anodic bonding in order to improve bonding quality [27] or in the fabrication of nanofluidic channels [28]. Recent work [29]

proved that  $\alpha$ -Si:H can facilitate the fabrication of ultrathin (15 nm) nonporous membranes for the filtration and separation of blood proteins with potential application in haemodialysis.

## 2. Experimental procedure

The deposition of  $\text{SiN}_x$ ,  $\alpha$ -Si:H and  $\alpha$ -SiC layers were performed using a plasma-enhanced chemical vapor deposition (PECVD) system (STS, Multiplex Pro-CVD). A schematic diagram of the equipment was presented by Chung et al in [30]. The unique characteristic of the system is that the plasma can be activated in two RF modes: at 380 kHz (LF) and/or at 13.56 MHz (HF). Another important characteristic of the equipment is that it offers the opportunity of selecting the power in a large range: between 0 and 600 W for HF mode and between 0 and 1 kW for LF mode. The depositions of the layers were performed using pure silane ( $\text{SiH}_4$ ), ammonia ( $\text{NH}_3$ ) and nitrogen ( $\text{N}_2$ ), for  $\text{SiN}_x$ , pure silane and argon (Ar) for  $\alpha$ -Si:H, pure silane, methane ( $\text{CH}_4$ ) and argon for  $\alpha$ -SiC.

For characterization of the deposited layers 4" silicon wafers, p-type, <100> crystallographic orientation, 1-10  $\Omega\text{cm}$  were used. The wafer was initially cleaned in piranha ( $\text{H}_2\text{SO}_4$ :  $\text{H}_2\text{O}_2$  in the ratio of 2:1) at 120 °C for 20 minutes, rinsed in DI water and spin-dried. The native oxide of the layer was removed by dipping the wafer for one minute in a classical BOE solution. The stress characterization of the  $\text{SiN}_x$  films was performed with a stress measurement system (KLA Tencor FLX-2320). The thickness of the films was measured with a refractometer (Filmetrics F50).

## 3. Fabrication of low stress PECVD layers

### 3.1. Influence of the deposition power

#### 3.1.1. Deposition of $\text{SiN}_x$ layers at low power in HF and LF mode

In most applications of PECVD, the HF (13.56 MHz) RF is the most common operation mode to deposit  $\text{SiN}_x$  film. The first deposition layers were fabricated at HF and the deposition power was changed from 20 W to 80 W, keeping the flow rates constant as follows:  $\text{SiH}_4/\text{NH}_3/\text{N}_2$  120/100/2200 sccm. The variations of residual stress and deposition rate of  $\text{SiN}_x$  layers at the above-mentioned range of power are shown in Figure 1. As shown the deposition rate increases with RF power. The increased RF power leads to higher electron density and therefore there is a relatively larger population of high-energy electrons. These high-energy electrons yield a higher ionization and dissociation rate, which consequently results in a higher deposition rate. Moreover, the power played an important role in determining the dominant film content - the layers deposited in high power process have a closer composition with the substrates due to the high dissociation rate of gases, which lead to more  $\text{N}^+$  species generated and consequently

result in increased incorporation of N bonding in the  $\text{SiN}_x$  film. This results in compressive stress due to the volume expansion of the  $\text{SiN}_x$  film [12]. Therefore, higher power brings high N bonding in the  $\text{SiN}_x$  film, and the higher volume expansion of the  $\text{SiN}_x$  film brings higher compressive stress, which compensates the tensile stress of the whole layer and leads to overall lower tensile stress. The result is that the deposition in HF mode, at low power (20-80 W), generates a tensile stress in the range of 120-150 MPa, the stress slowly decreases with the increasing of RF power, while the deposition rate presents a strong variation from 20 W (around 15 nm/min) to 80 W (around 70 nm/min).

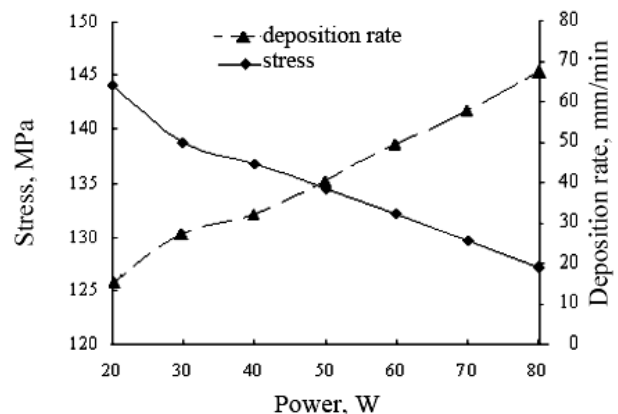


Fig. 1. Variation of the stress and deposition rate of  $\text{SiN}_x$  layer at low power in HF mode (13.56 MHz).

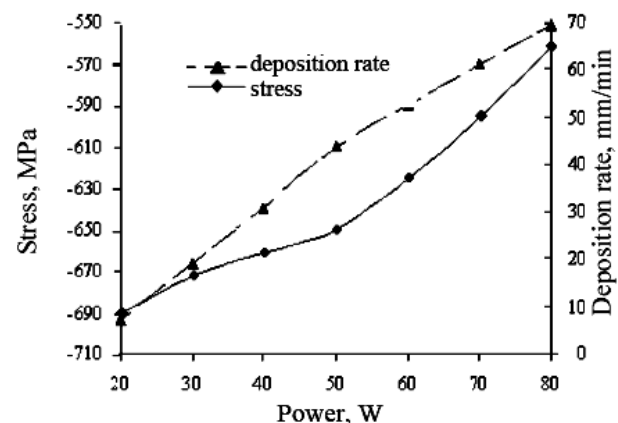


Fig. 2. Variation of the stress and deposition rate of  $\text{SiN}_x$  layer at low power in LF mode (380 KHz).

Fig. 2 shows the stress and deposition rate of  $\text{SiN}_x$  layers deposited using LF mode for a range of power between 20 W and 80 W. It is noted that for the LF deposition mode, the intrinsic stress state of the silicon nitride layer is compressive. The main reason is that at high frequency (13.56 MHz) only the electrons are able to follow the RF field while the ions are "frozen" in place by their heavier mass. In LF mode the ion bombardment is significantly higher, which not only enhance chemical reactions but also causes a low energy ion implantation that densifies the film and leads to a change of the stress state

from tensile to compressive [11]. However, from Figure 2, it can be seen that the RF power has little effect on  $\text{SiN}_x$  layer stress as an increase in ion bombardment is canceled out by a higher deposition rate. We can conclude that the deposition at LF and low power (20-80 W) results in a high value of compressive stress (600-700 MPa) while the deposition rate is increasing with the power (from 7.3 nm/min at 20 W to around 70 nm/min at 80 W). By alternating depositions in HF mode and LF mode or by using simultaneous both HF and LF mode we can achieve  $\text{SiN}_x$  layers with “zero residual stress”. The main disadvantage of such deposition is that, in order to achieve a homogenous layer, the thickness of the compressive and tensile layer must be as thin as possible. As a result a deposition at a low power (20 - 40 W) is desired. A characteristic of low power depositions, as we have previously shown, is low deposition rate.

### 3.1.2. Deposition at high power in HF mode

The observation that in HF mode the tensile stress decreases with the RF power while the deposition rate is significantly increased was further investigated in order to achieve a  $\text{SiN}_x$  layer with low stress (if it is possible, even “zero stress”) and high deposition rate. A series of experiments which deposited  $\text{SiN}_x$  layer in the power range of 100 W to 600 W have been completed. Figure 3 and Figure 4 show the variations of residual stress and deposition rate respectively with the power change. In these experiments, the pressure and temperature were kept constant at 900 mTorr and 300 °C respectively while several  $\text{SiH}_4/\text{NH}_3/\text{N}_2$  compositions were tested: 120/75/1200 sccm, 100/60/1500 sccm and 80/60/1700 sccm.

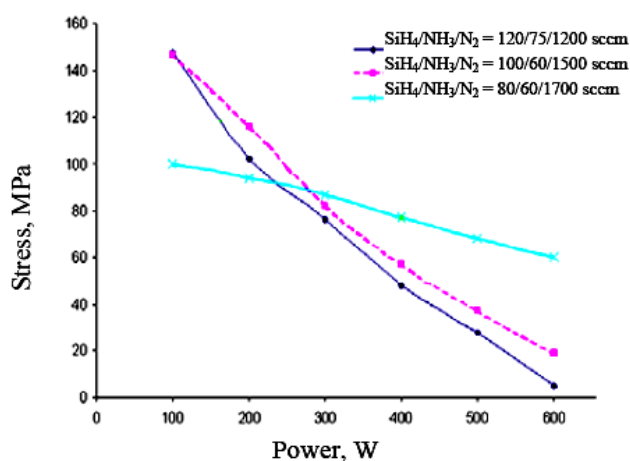


Fig. 3. Variation of  $\text{SiN}_x$  layer stress with the power in high power range for different  $\text{SiH}_4/\text{NH}_3/\text{N}_2$  compositions.

From the graphs, it can be observed that, with the increase of power from 100 W to 600 W, the deposition rate increases strongly from around 100 nm/min up to 250-320 nm/min while the residual stress decreases from 100-150 MPa tensile to 4-60 MPa. It can also be noticed that the variations of the deposition rate and residual stress are strongly correlated with the composition of the mixture gas

(this aspect will be presented in the next sections). For an increased concentration in  $\text{SiH}_4$  the deposition rate increases faster while the residual stress presents an accentuated decrease.

The higher power enhanced the plasma in the chamber, which subsequently yielded higher energy electrons. The increased energy of the electrons increases the dissociation of the main gases and as a result the deposition rate increases. Moreover, the dissociation energy of  $\text{N}_2$  is about 9.8 eV, whereas the bond-strength H-NH<sub>2</sub> is only about 4.6 eV, and the critical power to activate  $\text{NH}_3$  is only about 1/5 of that needed to activate  $\text{N}_2$ . Therefore, in the ultra-high power range, much more  $\text{N}_2$  have been activated and dissociated, which means more N atom will react with  $\text{SiH}_4$  and much more  $\text{SiN}_x$  will be generated. As previously explained, the decreasing stress value with the increase of power can be attributed to the high dissociation of  $\text{N}_2$  which led to more N species and resulted in an increased of N – Si bonding in  $\text{SiN}_x$  film. It is found that the residual stress of  $\text{SiN}_x$  layer decreases and the deposition rate increases with the increase of power. Moreover, the residual stress of silicon nitride layer deposited under the ultra-high power condition (600 W) can reach a low value (4 MPa) and is strongly related to the composition.

### 3.1.3. Deposition of $\alpha$ -Si:H at high power

For these experiments the process conditions were: temperature of 300 °C, pressure of 900 mTorr;  $\text{SiH}_4$  flow rate of 120 sccm and Ar flow rate of 700 sccm. The power of the HF generator was tuned between 100 W and 600 W, while the LF power was varied between 100 W and 1000 W. The deposition rate and residual stress of the  $\alpha$ -Si:H layers deposited using the two RF modes are shown in Figure 4 (a; b).

As was expected, for an increased power a high deposition rate is achieved for both RF modes. A high power can be associated with a high rate of gas dissociation, which leads to more reactive species in the plasma with direct effect on increasing the deposition rate. From Figure 4(a) it can be observed that the deposition rate and stress (compressive) values increase with the power for the HF mode. Meanwhile, for the other frequency mode, Figure 4(b) shows that there is a linear proportionality of the deposition rate with the LF power. The strong dependence of the deposition rate on the power can be explained by the increased dissociation of  $\text{SiH}_4$ . It can also be seen in Figure 4(b) that for this mode the stress is not significantly influenced by the deposition power as only small fluctuations seem to occur in a small range of values between -350 MPa and -300 MPa (the measurement errors may also play an important role). This relatively constant stress in the LF mode is a result of ion bombardment that characterizes plasma at low frequency. At high frequency (more than 1 MHz) the ions cannot follow the frequency due to their inertial mass.

For this reason, deposition at LF is associated with a bombardment of the thin layer with effect on densification and stress. Comparing between the two graphs of Figure 4(a) and Figure 4(b) it can be seen that the lowest residual stress levels can be achieved in the HF mode by employing

low HF power. Unfortunately, this also leads to a dramatically lower deposition rate, which is undesirable.

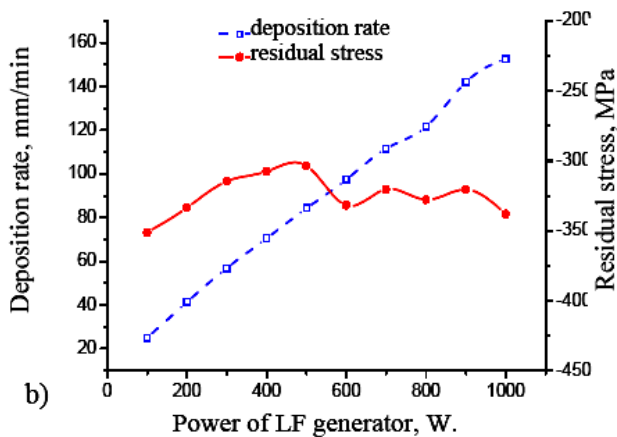
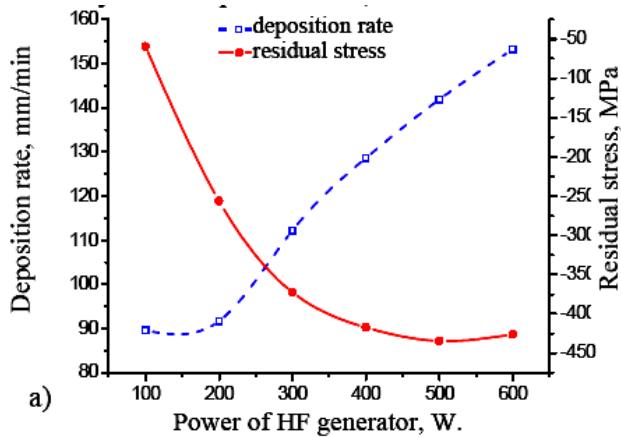


Fig. 4. The dependence of the stress and the deposition rate on deposition power for: a) HF, and b) LF modes.

### 3.1.4. Deposition of $\alpha$ -SiC at high power

The influence of the RF power  $P$  was studied in both the HF and LF modes at a pressure  $p$  of 1100 mTorr. All the other deposition parameters ( $T$  and gas flow rates) have been kept constant at the values specified in the previous sub-section while the RF power was varied between 0 W and 600 W for the HF mode and between 0 W and 1000 W for the LF mode. For the HF mode the variation of deposition rate and stress are presented in Figure 5 [31]. The almost linear increasing of the deposition rate with the HF power can be explained by the increased dissociation of reactant gasses. However, at higher HF power (greater than 300 W) level, the reaction is limited by the transport of reactive species. Characteristic to the deposition in HF mode is the low stress value. For a wide range of power the variation of the stress is between 50 MPa tensile and 70 MPa compressive, with achieving the “zero point” at 110 W. For these depositions, the refractive index was almost constant in the range between 2.5 and 2.6 while the uniformity of the deposition and uniformity of the refractive index was below 1.5%.

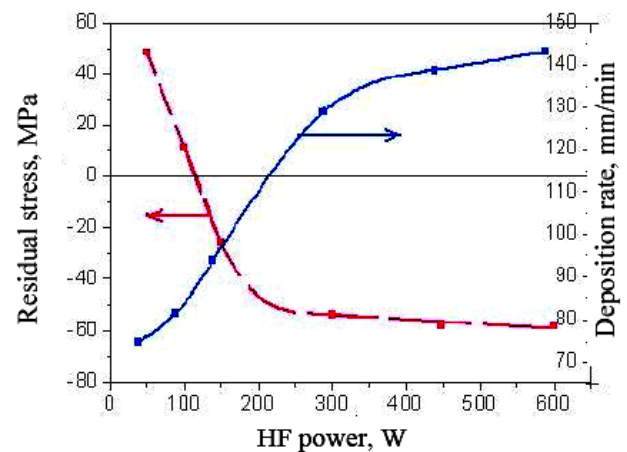


Fig. 5. Influence of power for HF mode on the stress and the deposition rate.

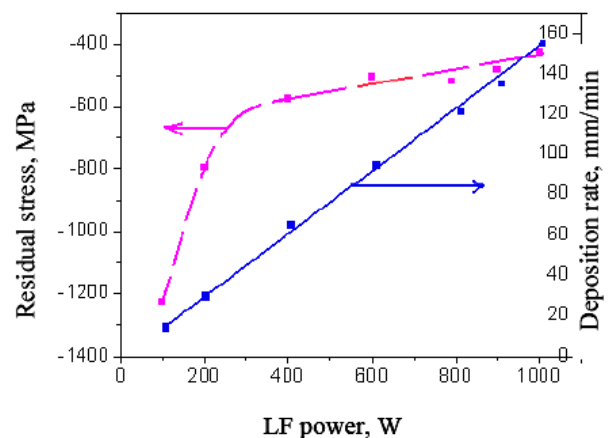


Fig. 6. Influence of power for LF mode on the stress and the deposition rate.

The variation of the deposition rate and stress of  $\alpha$ -SiC films in LF mode are presented in Figure 6 [31]. We noticed that, for LF mode, there is an almost linear relationship between the deposition rate and the power. The stress is compressive with high values for low power and become almost constant values after the power rich 300 W (around 500 MPa). This variation of the stress can be explained by the densification of the layer achieved by ion bombardment. We can conclude that, for stress considerations, by tuning the power appropriately in the HF mode, the residual stress can reach near zero values. Moreover, the deposition rate in HF mode is increased (for the same value of the applied power) due to the better dissociation of the gasses.

## 3.2. Influence of the reactor pressure

### 3.2.1. Influence on the deposition of $\text{SiN}_x$ layers

Pressure is another critical parameter which will greatly influence the characteristic of  $\text{SiN}_x$  layers. In this part, a series of  $\text{SiN}_x$  layers were deposited under different

pressures from 700 mTorr up to 1100 mTorr, whilst other parameters were kept constant: SiH<sub>4</sub>: 120 sccm; NH<sub>3</sub>: 75 sccm; Power: 600 W; N<sub>2</sub>: 1150 sccm. Figure 7 shows how the deposition rate and residual stress changed with pressure. [32, 33] These two graphs indicate that pressure has a great effect on the SiN<sub>x</sub> deposition rate and stress. The reason may be that the decreasing pressure results in an increase in electron energy, which subsequently leads to an increase in N to SiH<sub>3</sub> radical ratio, namely the decrease of Si/N ratio. This interpretation is consistent with the enhanced concentration of N-H bonds resulting from a pressure decrease. Moreover, pressure has a great influence on plasma stabilization. Therefore, from the graphs, it can be seen that at 700 mTorr pressure, the deposition rate and stress change coming from N<sub>2</sub> flow rate are larger than the other two. Furthermore, the uniformity of 700 mTorr is typically up to 10%, larger than those of 900 mTorr and 1100 mTorr, which are 2% and 1% respectively. However, in the 1100 mTorr pressure, the residual stress is higher. It can be concluded from the above analysis that a pressure around 900 mTorr would be optimal for SiN<sub>x</sub> deposition due to its stable plasma and low residual stress generated. [32, 33].

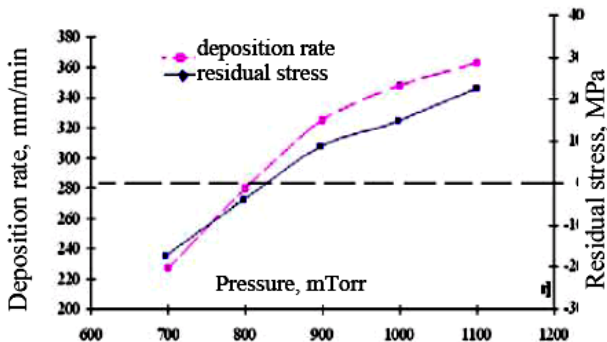


Fig. 7. Variation of residual stress and deposition rate for high power (600 W) in HF mode in SiN<sub>x</sub> layer with pressure.

### 3.2.2. Influence on the deposition of $\alpha$ -Si:H layers

The experimental conditions were: temperature of 300 °C, power of 450 W, SiH<sub>4</sub> flow rate of 120 sccm and Ar flow rate of 700 sccm. In this case, pressure was varied between 600 mTorr and 1000 mTorr with a step of 100 mTorr. The results for both HF and LF modes are shown in Figures 8(a) and 8(b), respectively. Figure 8(a) shows that deposition rate varies between 100 and 135 nm/min, with its maximal point at 900 mTorr in the HF mode, while the induced stress also increases remarkably from -100 MPa to -490 MPa when increasing pressure. At an increased pressure the mean free path distance between the molecules of reactant gases, charged and energetic species is reduced and the number of effective collisions increases significantly, leading to additional association as well as dissociation. In a first phase, the number of increased molecular association aids the

deposition and, hence, the deposition rate increases. In a second phase, however, if the pressure continues to increase, although the number of collisions continues to increase, but the greatest majority will be less and less related to reaction(s) with the substrate; as a result the deposition rate decreases after reaching a local maximum. Fig. 8(b) shows that for both HF and LF modes, the residual stress magnitude decreases with pressure, but its values are still much higher than those which can be obtained in the HF mode. At the same time, the HF mode also provides more attractive deposition rates than the LF mode. Therefore, a low pressure of around 700 mTorr (in the HF mode) was chosen to achieve the very low stress and proper high deposition rate  $\alpha$ -Si:H layers.

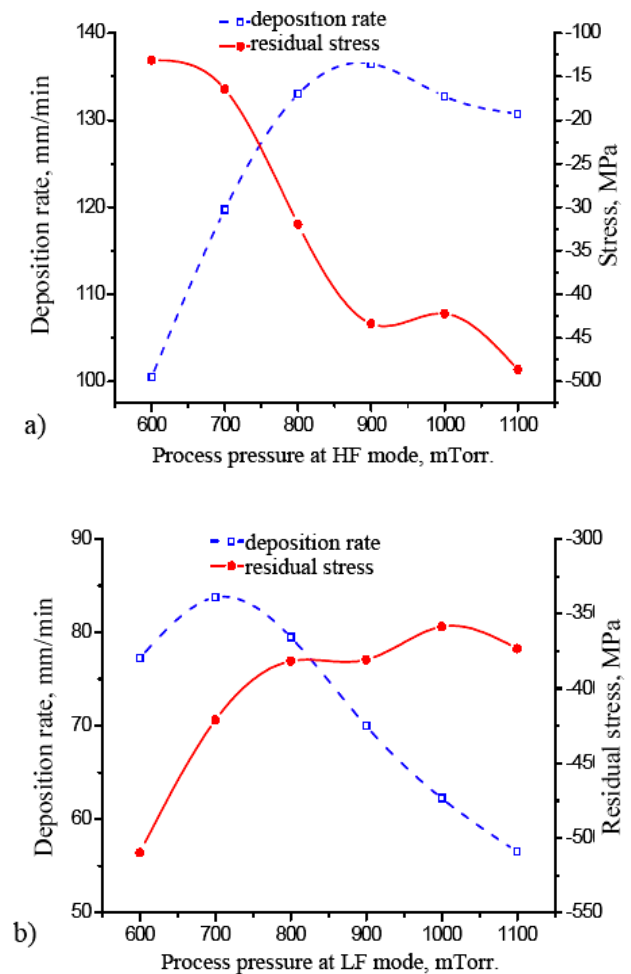


Fig. 8. The dependence of the stress and the deposition rate on deposition pressure for: a) HF, and b) LF modes.

### 3.2.3. Influence on the deposition of $\alpha$ -SiC layers

The pressure  $p$  of the chamber was varied between 500 mTorr and 1400 mTorr, while the other parameters were maintained constant: deposition temperature  $T$  of 300 °C, RF power  $P$  at 150 W in HF mode, and gas flow rates of SiH<sub>4</sub>, CH<sub>4</sub> and Ar at 45, 300 sccm and 700 sccm, respectively. The most important observed element was that deposition uniformity is strongly dependent on the

pressure in the chamber (Fig. 9) [31]. In the low pressure regime (below 800 mTorr) the non-uniformity presents high values, the recommended pressure range for the deposition of films with very good uniformity being from 900 mTorr up to 1400 mTorr. A reason can be a high pumping speed that may determine an extremely large velocity of the gas molecules so that most of the gas injected from the shower above the wafer will no longer follow the normal flow pattern. Instead, most of the gas will be increasingly concentrated towards the edges of the wafer in order to minimize the flow path towards the exhaust, as imposed by the high pumping speed. This modified flow pattern concentrated predominantly at the wafer edge will, in turn, lead to an increased deposition rate in that region. A second noticed aspect was the variation of the average deposition rate with the pressure (Fig. 9) [31]. Low pressure values in the chamber determine a low concentration of reactive species, so that with increasing pressure, more reactive species are generated and the deposition rate increases.

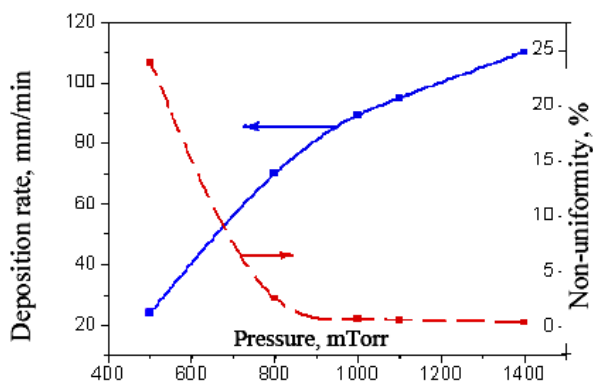


Fig. 9. Influence of the pressure on the deposited film thickness non-uniformity variation and the deposition rate

### 3.3. Influence of the substrate temperature

For these experiments the process conditions were: power of 300 W (LF and HF), pressure of 900 mTorr, SiH<sub>4</sub> flow rate of 120 sccm and Ar flow rate of 700 sccm. The experiments were carried out at four different temperatures: 200 °C, 250 °C, 300 °C and 350 °C. Figures 10(a) and 10(b) represent the stress and deposition rate for HF and LF modes at a deposition power of 300 W. Relatively similar variations with the deposition temperature were observed for other RF power levels, too. As Figures 10(a) and 10(b) show, the residual stress is compressive for both RF modes. While for LF mode the stress varies in a wide range (between 310 and 450 MPa) with increased values at low temperatures, for HF mode a significant low stress value of 250 MPa was achieved at 200 °C. Usually, an increased temperature of the substrate accelerates the reaction rate on the substrate surface and a high deposition rate can be achieved. However, in the HF mode the opposite was observed: the deposition rate decreased dramatically (from 140 nm/min to 105 nm/min) when the substrate temperature was increased from 200 °C to 250 °C. This counter-intuitive behavior can be due to the generation of “microcrystalline”  $\alpha$ -Si:H ( $\mu$ c-Si), as reported previously [29, 30]. It can also

be noticed that much higher deposition rates are obtained in the HF mode than in the LF mode. An additional set of experiments was carried out at 100 W in the HF mode with temperature variations, and the results are shown in Figure 10(c). As expected, in this case lower stress values are obtained than those shown in Figures 10(a) and 10(b). Specifically, a tensile stress (40 MPa) was generated in the  $\alpha$ -Si:H thin layer deposited at 200 °C, while the deposition rate at different temperatures varied only between 85 nm/min and 95 nm/min. Therefore, the combination of a low deposition temperature of 200 °C and low power of around 100 W in HF mode can provide low residual stress (around “zero” value) and an acceptable deposition rate of  $\alpha$ -Si:H thin layers.

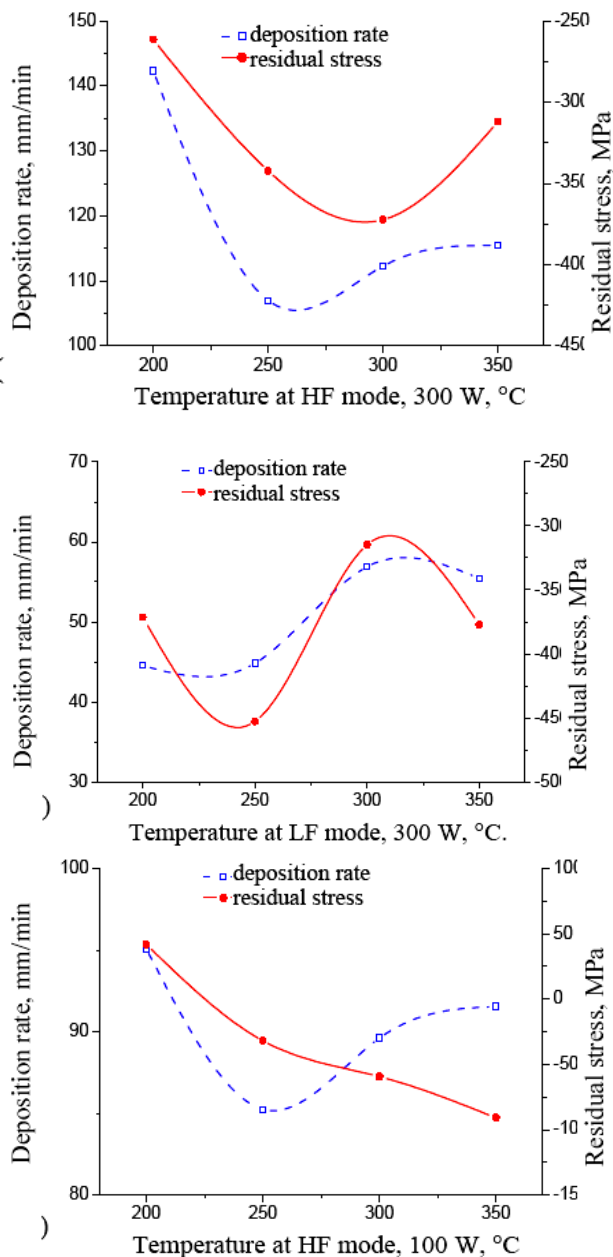


Fig. 10. The dependence of the stress and the deposition rate on deposition temperature for: a) HF, b) LF modes, when the applied power is 300 W, and c) for an applied HF power of 100 W

The influence of temperature on  $\alpha$ -SiC layers was studied between 200 °C to 400 °C, while the other parameters were kept constant with: pressure at 1100 mTorr, power at 150 W in HF mode, gas flow rates SiH<sub>4</sub>/CH<sub>4</sub>/Ar 45 sccm/ 300 sccm/ 700 sccm. Experiments were also performed for LF mode but no relevant variations with the temperature of the deposition rate, stress and uniformity were observed. For the HF mode a slow decreasing of deposition rate (less than 10%) with the increasing of temperature was noticed. This suggests that the dissociation of molecules and radicals absorbed on the substrate surface (enhanced by electron bombardment) and the re-evaporation of absorbed molecules and radicals (enhanced by the Ar ions impinging onto the substrate surface) are relatively in equilibrium. The increased number of Ar ions intruded onto the substrate surface at higher temperature presents an important effect on the stress variation. As presented in Figure 11 [31], with the increasing of temperature, the stress become tensile (while the refractive index was almost constant at 2.6). As a result, the recommended range of temperature for depositing low stress  $\alpha$ -SiC depositions on PECVD reactors, is between 300 °C and 400 °C.

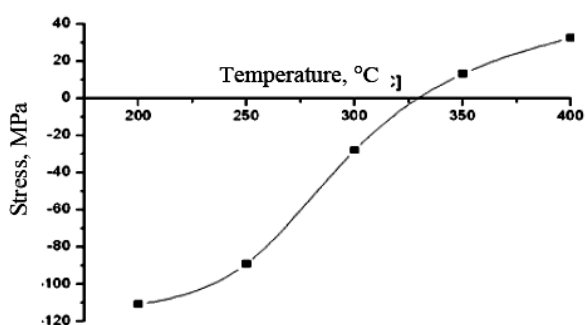


Fig. 11. Influence of the temperature on residual stress in HF mode.

#### 4. Applications

SiN<sub>x</sub> layer can be used in cell culture applications [34, 35] an image with a fibroblast cell culture on a SiN<sub>x</sub> membrane is presented in Figure 12. Recent works shows application of SiN<sub>x</sub> membrane in high throughput drug screening process [36]. This aspect can be explained by the amine (NH<sub>2</sub>) groups presented at SiN<sub>x</sub> surface that promote the interaction between the cell membrane and substrate. Relatively similar results were achieved also using amorphous SiC membranes [31], but only after the surface were treated with NH<sub>4</sub>F.

Low stress a:Si layer can be used micropatterning of glass [37] for microfluidic applications [38, 39] being a relatively chip comparing with Cr/Au masking layers presented in [40, 41]. Meanwhile, doped with aluminum can be used as electrode in dielectrophoretic chips [42, 43]. Moreover, the a:Si can be dry etch using XeF<sub>2</sub>, an etching process with a high selectivity to thin layers such as SiC, SiO<sub>2</sub> or even photoresist. As a result, the low stress a:Si layer can be used as sacrificial layer [44] for fabrication of free standing structures using surface micromachining.

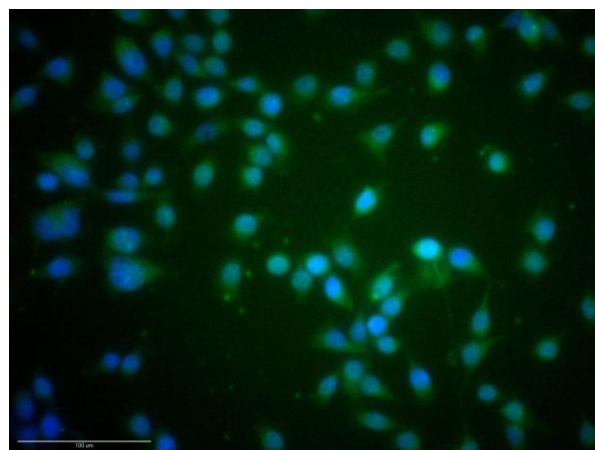


Fig. 12. Fibroblast cell culture on a SiN<sub>x</sub> membrane.

#### 5. Conclusions

The paper presents an analysis of the effects of the main process parameters on deposition in PECVD systems. The main parameters are customized in order to achieve a low value of the residual stress, almost zero. The resulted process conditions to fabrication SiN<sub>x</sub> layers with low stress there are: RF power 600 W alternating HF and LF mode, pressure 800 mTorr and flow rates N<sub>2</sub>/NH<sub>3</sub>/SiH<sub>4</sub>: 1200/30/60 sccm. The same customization was made for deposition of  $\alpha$ -Si:H layers and  $\alpha$ -SiC layers. The process parameters obtained were: RF power 100 W, in HF mode, pressure 600 mTorr and temperature 250 °C for  $\alpha$ -Si:H layers, and respectively, RF power 150 W, in HF mode, pressure 700 mTorr and flow rates Ar/CH<sub>4</sub>/SiH<sub>4</sub>: 700/900/50 sccm and temperature 325 °C for  $\alpha$ -SiC layers.

#### References

- [1] J. Y. M. Lee, K. Sooriakumar, M. M. Dange, *Thin Solid Films* **203** 275 (1991).
- [2] A. Neumann, T. Reske, M. Held, K. Jahnke *J. Mater. Sci.: Mater. Med.* **15**, 1135 (2004).
- [3] D. R. Ciarlo, *Biomed. Microdevices* **4**(1) 63 (2002).
- [4] P. R. Scheeper, W. Olthuis, P. Bergveld, *Sensors and Actuators A* **40**, 179 (1994).
- [5] P. Schmid, M. Orfert, M. Vogt, *Surface and Coating Technology* **98**, 1510 (1998).
- [6] W. J. Dauksher, D. J. Resnick, S. M. Smith, S. V. Pendharkar, H. G. Tompkins, K. D. Cummings, P. A. Seese, P. J. S. Mangat, J. A. Chan, *J. Vac. Sci. Technol. B* **15**, 2232 (1997).
- [7] N. Chitica, M. Strassner, J. Daleiden *Appl. Phys. Lett.* **77**, 202 (2000).
- [8] H. Gukel, D. Burnst, C. Rutigliano, E. Lovell, B. Choi *J. Micromech. Microeng.* **2**, 86 (1992).
- [9] D. Lapadatu, A. Pyka, J. Dziuban, R. Puers *J. Micromech. Microeng.* **6**, 73 (1996).
- [10] A. Tarraf, J. Daleiden, S. Irmer, D. Prasai, *MEMS J. Micromech. Microeng.* **14**, 317 (2004).

- [11] E P van de Ven, I. W. Connick, A..S. Harrus Proc. of the VLSI Multilevel Interconnection Conference (VMIC), Santa Clara, CA, 94-101. Stress investigation of PECVD 1990
- [12] K. D. Machenzie, B. Reelfs, M. W. DeVre, R. Westerman, D. J. Johnson *Chip* **10**, 26 (2004).
- [13] M. J. ,Loboda J. A. Seifferly *J. Mater. Res.* **11**, 391 (1996).
- [14] T. H. T. Wu, R. S. Rosler, *Solid State Technology* 65-72, 1992
- [15] E. Sleenckx, M. Schaekers, X. Shi, E. Kunnen, B. Degroote, M. Jurczak, M. de Potter de ten Broeck, E. Augendre, *Microelectronics Reliability* **45**, 865 (2005).
- [16] P. Louro, M. Vieira, A. Fantoni, M. Fernandes, C. N. de Carvalho, G. Lavareda, *Sensors and Actuators A* **123-124**, 326 (2005).
- [17] D. Knipp, R. A. Street, H. Stiebig, M. Krause, J. P. Lu, S. Ready, J. Ho, *Sens Actuators A* **128**(2), 333 (2006).
- [18] L. Dong, R. Yue, L. Liu, S. Xia, *Sens Actuators A* **116**(2), 257 (2004)
- [19] H. C. Lim, B. Schulkin, M. J. Pulickal, S. Liu, R. Petrova, G. Thomas, S. Wagner, K. Sidhu, J. F. Federici, *Sens Actuators A* **119**(2), 332 (2005).
- [20] R. T. Howe, R. S. Muller, *Sensors Actuators A* **4**, 447 (1983).
- [21] C. Iliescu, J. Jing, F. E. H. Tay, J. M. Miao, T. T. Sun *Surf. Coat. Technol.* **198**(1-3), 314 (2005).
- [22] C. Iliescu, D. P. Poenar, M. Carp, F. C. Loe, *Sens Actuators B* **123**(1), 168 (2007).
- [23] C. Iliescu, *J. of Microelectronics, Electronic Components and Materials* **36**(4), 204 (2006).
- [24] C. Iliescu, L. M. Yu, G. L. Xu, F. E. H. Tay, *J. Microelectromechl Syst* **15**(6), 1506 (2006).
- [25] X. Jin, I. Ladabaum, B. T. Khuri-Yakub, *J. Microelectromechl Syst* **7**(3), 295 (1998).
- [26] C. D. White, G. Piazza, P. J. Stephanou, A. P. Pisano *Sens Actuators A* **134/1** 239-244 (2007).
- [27] J. Wei, C. K. Wong, L. C. Lee, *Sens Actuators A* **113**(2), 218 (2004).
- [28] V. G. Kutchoukov, F. Laugere, W. van der Vlist, L. Pakula, Y. Garini, A. Bossche, *Sens Actuators A* **114**(2-3), 521 (2004).
- [29] C. C. Striemer, T. R. Gaborski, J. L. McGrath, P. M. Fauchet, *Nature* **445**, 749 (2007).
- [30] C. K. Chung, M. Q. Tsai, P. H. Tsai, C. Lee, *J. Micromech. Microeng.* **15**(1), 136 (2005).
- [31] C. Iliescu, B. T. Chen, D. P. Poenar, Y. Y. Lee, *Sensors and Actuators B*, **129**(1), 404 (2008).
- [32] P. L. Ong, J. Wei, F. E. H. Tay, C. Iliescu, *J. Phys.: Conf. Ser.* **34**, 764 (2006).
- [33] C. Iliescu, F. E. H. Tay, J. Wei, *J. Micromech. Microeng.* **16**(4), 869 (2006).
- [34] M. Ni, W. H. Tong, D. Choudhury, N. A. A. Rahim, C. Iliescu, H. Yu, *International Journal of Molecular Sciences*, **10**(12), 5411 (2009).
- [35] C. Iliescu, J. Wei, B. Chen, P. L. Ong, *Science and Technolog*, **11**(2), 167 (2008).
- [36] S. Zhang, W. H. Tong, B. Zheng, T. A. K. Susanto, L. Xia, C. Zhang, A. Ananthanarayanan, X. Tuo, S. R. Binte R. Jia, C. Iliescu, K. H. Chai, M. McMillian, S. Shen, H. L. Leo, Yu H., *Biomaterials*, **32**(4), 1229 (2011).
- [37] C. Iliescu, B. T. Chen, J. M. Miao, *Sensors and Actuators A*, **143**(1), 154 (2008).
- [38] F. S. Iliescu, A. R. Sterian, E. Barbarini, M. Avram, C. Iliescu, *UPB Scientific Bulletin-Series A-Applied Mathematics and Physics*, **71**(4), 21 (2009).
- [39] D. P. Poenar, C. Iliescu, M. Carp, A. J. Pang, K. J. Leck, *Sensors and Actuators A*. **139**(1-2), 162 (2007).
- [40] C. Iliescu, F. E. H. Tay, J. Miao, *Sensors and Actuators A*, **133**(2), 395 (2007).
- [41] F. E. H. Tay, C. Iliescu, J. Jing, J. Miao, *Microsystem Technologies*, **12**(10-11), 935 (2006).
- [42] C. Iliescu, G. Tresset, G. L. Xu, *Biomicrofluidics*, **3**(4), 044104 (2009).
- [43] C. Iliescu, D. P. Poenar, S. T. Selvan, *Journal of Micromechanics and Microengineering*, **20**(2), art. no. 022001 (2010).
- [44] C. Iliescu, B. T. Chen, *J. Micromech. Microeng.* **18**(1), art. no 15024 (2008).

---

\*Corresponding author: slavko.amon@fe.uni-lj.si